Journal of Sound and Vibration (1999) **224**(1), 101–122
Article No. jsvi.1999.2172, available online at http://www.idealibrary.com on IDEAL®

ON THE EFFECTIVE CONTROL OF TORSIONAL VIBRATIONS IN DRILLING SYSTEMS

R. W. TUCKER AND C. WANG
*Department of Physics, Lancaster University, LA*1 4*YB, England*

(*Received* 3 *July* 1998, *and in final form* 27 *January* 1999)

This paper analyses a control mechanism designed to significantly ameliorate the sustained excitation of torsional relaxation oscillations (slip–stick) due to frictional torques generated by an active bit during drilling operations with an extended drill-string. The proposed mechanism of *torsional rectification* is compared with existing soft-torque devices in a series of mathematical models. Both analytic and numerical simulations indicate that many of the volatilities suffered by existing soft-torque feedback approaches used to combat slip–stick can be eliminated by the alternative proposed here.

1. INTRODUCTION

A major concern in the oil drilling industry remains the high cost of drill-bit failures due to the build up of damaging vibrations while drilling for oil. Despite continuing efforts to control such vibrations there is evidence that the detailed nature of drill-string dynamics is still not fully understood. This may be partly due to the fact that successful modelling of an active drilling assembly (Figure 1) is an exceedingly complex problem. Progress has been made by attempting to isolate those aspects that can be simply modelled with the data available while being fully aware of the limitations inherent in the neglect of the coupling between the axial, lateral and torsional modes of vibration of the drill-string induced by external forces and torques [1–4]. These external influences include interactions of the string with its environment, interactions of the drill-bit with the rock face, interactions induced by stabilisers on the bottom-hole assembly, and forces and torques transmitted by the top drive and rotary. One of the severest sources of torsional vibration is the reaction to non-linear torque-friction at the rock–bit interface. Below critical rotational speeds this interaction can trigger a build up of self-sustained torsional "slip–stick" in which the whole drill-string is torsionally excited while the drill-bit alternatively slips and comes to rest. Such vibrations often lead to unsustainable torques in the drill-string. Efforts [5–7] to ameliorate the build up of torsional energy in this form have focussed on various feedback devices that control the speed and torque of the

0022–460X/99/260101 + 22 $30.00/0

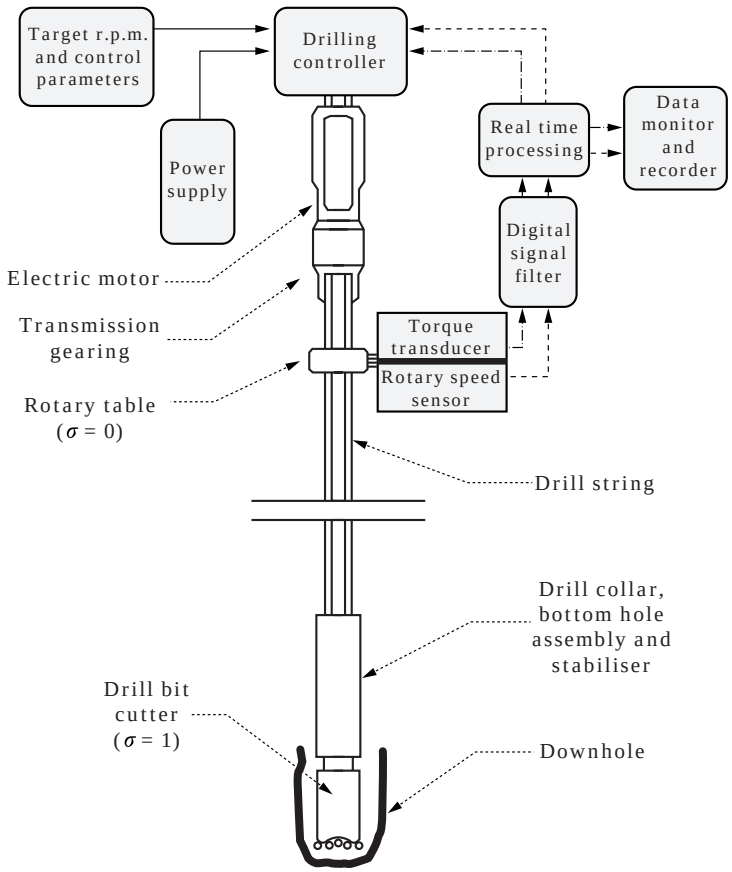

Figure 1. Schematic representation of a drilling assembly. The model discussed in this article refers to the dynamics of the region between $\sigma = 0$ and $\sigma = 1$ with the torques arising from the friction induced between the bit and the down-hole rock formation and the drive from the drilling controller. The latter contains active feedback control from the torque transducer and rotary speed sensor near the surface rotary table. In conventional "soft-torque" feedback control the signal filter is used to remove low frequency torsional signals in order to effect stabilisation in addition to standard high frequency noise filtering. In the "torsional rectification" described in this article only the latter is employed thereby enlarging the window of torsional energy absorption at the rotary.

drive at the well-head [8, 9]. Torque feedback devices [8] attempt to reduce the effective reflection coefficient for torsional energy at the rotary. Although details vary, they are essentially based on the frequency analysis of simultaneously pre-recorded torque and rotary speed data, specific to individual sites. Such devices are usually optimised for generic operation and often require repeated retuning in the field as the drilling characteristics vary. Such retuning carries the hazard of sometimes exacerbating the situation. Furthermore in certain situations increasing conventional torque feedback can destabilise a dynamical state and actually accelerate the transition to slip–stick.

A more recent proposal [10] attempts to circumvent these problems by actively monitoring the current and voltage of the rotary drive motor and constructing a device to control the stability of the system regarded as a pair of coupled,

damped, forced torsional pendula. This approach is free from active torque monitoring but is optimised to control the first few torsional modes of the drill-string. This may be a limitation since the slip–stick vibrations carry a rich harmonic structure and a linear stability analysis that ignores the effect of the continuum nature of the drill-string is at best a guide to the non-linear dynamical effects of torque friction.

This article addresses the problem of the volatility of existing torque feedback controllers and explores an alternative mechanism that is felt to circumvent the need for persistent retuning. The basic idea stems from the recognition that arbitrary amplitude torsional disturbances on the drill-string (modelled as a space curve rotating in an axisymmetric configuration) satisfy a simple linear wave equation whose general solution permits the identification of both "up" and "down" moving components. The consequences of maintaining the energy of the "down" component constant in the presence of the non-linear dynamic boundary conditions induced by the presence of dynamic friction between the drill-bit and the rock face (Figure 8) is explored. One finds that this can be achieved by monitoring the contact torque between the drill-string and the rotary drive and by introducing a compensating drive torque that "rectifies" the "up-" moving torsional waves on the drill-string. To test these ideas, two simple models have been implemented in this paper. The first model explores the absorption and reflection of monochromatic torsional waves at the rotary of a drilling assembly, generated by a prescribed source of up-moving waves at the drill-bit. In the second model the finite time of propagation of the torsional waves along the drill-string is ignored and the system regarded as a simple forced torsional pendulum with non-linear torques generated by the drill-bit*.

2. TORSIONAL RECTIFICATION

Models of torsional vibrations of a vertical drill-string driven by a source of controlled torque at the well head and subject to torsional friction at the bit (see Figure 1) are analyzed. The purpose is to understand the volatility of traditional soft-torque feedback mechanisms and suggest a radically new approach based on the theory of travelling torsional waves. The idea is most readily understood in a limit where the bit reaction with the rock formation is regarded as a prescribed source of torsional disturbances that reflect from the top rotary. In the following the basic ideas are presented in units designed to simplify the presentation and have general applicability to different field operations. Since the ratio of the diameter to the length of a typical drill-string is often less than that of a human hair a drill-string is modelled by an open space-curve. Points along the drill-string are identified by σ in units of L where L is the length of any drill-string. Time η is measured in terms of the corresponding transit time of torsional disturbances from the bit to the top rotary. (Thus in these units the speed of torsional waves is one). Torques and control parameters are scaled appropriately

*These models are the precursors of more general simulations [11] that include the continuum nature of the drill-string and will be presented elsewhere.

to dimensionless units. Results are immediately interpretable in terms of factors scaling operational data such as "weight on bit' in KIPS and target RPM.

Let $\phi(\sigma, \eta)$ be the angular displacement of the drill-string (relative to a fixed frame at the well-head) at a point labelled σ at time η and satisfying the torsional wave equation

$$\ddot{\phi}(\sigma, \eta) - \phi''(\sigma, \eta) = 0, \tag{1}$$

where

$$\dot{\phi}(\sigma, \eta) \equiv \partial\phi(\sigma, \eta)/\partial\eta, \quad \phi'(\sigma, \eta) \equiv \partial\phi(\sigma, \eta)/\partial\sigma, \quad 0 \leqslant \sigma \leqslant 1,$$

with $\sigma = 0$ denoting the connection of the drill-string with the rotary and $\sigma = 1$ denoting the location of the bit interaction with the rock formation.

The torsional displacement is subject to the dynamical boundary conditions

$$\ddot{\phi}(0, \eta) = \mathcal{F}_0(\dot{\phi}(0, \eta), \phi'(0, \eta), \phi(0, \eta), \eta), \tag{2}$$

$$\ddot{\phi}(1, \eta) = \mathcal{F}_1(\dot{\phi}(1, \eta), \phi'(1, \eta), \phi(1, \eta), \eta) \tag{3}$$

for some functions $\mathcal{F}_0$ and $\mathcal{F}_1$ determined by drive and friction torques at the rotary and bit respectively.

To analyse the dynamic interaction between the rotary and the torsional waves on the drill-string one considers the general solution:

$$\phi(\sigma, \eta) = \mathcal{U}(\eta + \sigma) + \mathcal{D}(\eta - \sigma) \tag{4}$$

to the wave equation (1) in terms of an arbitrary "up-moving wave" $\mathcal{U}(\eta)$ and an arbitrary "down-moving wave" $\mathcal{D}(\eta)$. The time and spatial derivatives of $\phi(\sigma, \eta)$ are

$$\dot{\phi}(\sigma, \eta) = \dot{\mathcal{U}}(\eta + \sigma) + \dot{\mathcal{D}}(\eta - \sigma), \quad \phi'(\sigma, \eta) = \dot{\mathcal{U}}(\eta + \sigma) - \dot{\mathcal{D}}(\eta - \sigma), \tag{5, 6}$$

respectively. Since the contact torque at any point on a typical drill-string is proportional to the spatial derivative $\phi'(\sigma, \eta)$, $\dot{\mathcal{D}}$ describes the transmission of torque to the bottom assembly. To maintain a steady drilling operation with a constant target rotary speed with a constant twist along the drill-string it is desirable to maintain this close to a constant. However in the presence of the up-moving waves, $\dot{\mathcal{D}}$ also carries the vibration torques reflected from the rotary which are in turn reflected from the bottom assembly. Without further damping torsional vibrational energy can build up thereby leading to instability. One argues that monitoring the quantity $\Psi(\eta)$ defined by

$$\Psi(\eta) \equiv \dot{\phi}(0, \eta) - \phi'(0, \eta) = 2\dot{\mathcal{D}}(\eta), \tag{7}$$

obtained from equations (5) and (6), affords a valuable and practical means of controlling unwanted torsional vibration. The top rotary speed $\dot{\phi}(0, \eta)$ is regularly monitored while $\phi'(0, \eta)$ could be measured by a piezoelectric transducer attached to a top segment of the drill-string.

The top boundary condition ($\sigma = 0$) for some choice of control torque T_{motor} follows from Newton's law aplied to the rotary as:

$$\ddot{\phi}(0, \eta) = T_{motor}(\eta) + G_{top}\phi'(0, \eta), \tag{8}$$

where $G_{top} > 0$ is proportional to the torsional rigidity of the drill-string. The standard top-drive control attempts to maintain a constant rotary speed Ω_0 via the following form of the motor torque:

$$T_{motor}(\eta) = \kappa_p\dot{\xi}(\eta) + \kappa_i\xi(\eta), \tag{9}$$

where κ_p and κ_i are some positive control parameters (known as the proportional and integral gain variables respectively) and

$$\dot{\xi}(\eta) = \Omega_0 - \dot{\phi}(0, \eta), \quad \xi(\eta) = \Omega_0\eta - \phi(0, \eta) + \xi_0, \tag{10, 11}$$

for some constant ξ_0 denote the departure of the angular velocity and displacement respectively of the drill-string at the rotary from their stationary (target) values. In view of the comments above it is proposed to modify T_{motor} with an additional negative feedback proportional to $\Psi(\eta)$ so that

$$T_{motor}(\eta) = \kappa_p\dot{\xi}(\eta) + \kappa_i\xi(\eta) - \lambda\Psi(\eta), \tag{12}$$

where $\lambda \geqslant 0$ is a new control parameter.

In order to analyse such a control the effect of an incident torsional harmonic wave on the rotary is explored. Two base data sets for comparison based on different parameters used in typical drilling operations are adopted. Base data set 1 contains the parameters $\{\kappa_p = 1{\cdot}314,\ \kappa_i = 0{\cdot}08336,\ G_{top} = 0{\cdot}4836\}$ and base data set 2 contains the parameters $\{\kappa_p = 0{\cdot}3658,\ \kappa_i = 0{\cdot}1672,\ G_{top} = 0{\cdot}5765\}$. The dynamics of the bit in this approach are relegated to a prescribed source of torsional harmonics. A solution describing a harmonic wave of angular frequency ω and amplitude $A_{\mathcal{U},\omega}$ incident on the rotary from below, and reflected with amplitude $A_{\mathcal{D},\omega}$ is determined by writing

$$\phi(\sigma, \eta) = A_{\mathcal{U},\omega}\sin(\omega(\eta + \sigma)) + A_{\mathcal{D},\omega}\sin(\omega(\eta - \sigma) + \alpha_\omega) + \Omega_0\eta + C_0\sigma, \tag{13}$$

which solves (1). The constants C_0, α_ω and the ratio $A_{\mathcal{D},\omega}/A_{\mathcal{U},\omega}$ follow immediately from equations (8)–(12):

$$C_0 = (\lambda\Omega_0 - \kappa_i\xi_0)/(G_{top} + \lambda), \tag{14}$$

$$\alpha_\omega = \tan^{-1}\left(\frac{2\omega(\kappa_i - \omega^2)(G_{top} + \lambda)}{\omega^4 - (2\kappa_i + (G_{top} - \kappa_p)(G_{top} + \kappa_p + 2\lambda))\omega^2 + \kappa_i^2}\right) \tag{15}$$

and

$$A_{\mathcal{D},\omega} = \frac{\kappa_i - \omega^2}{(\kappa_i - \omega^2)\cos(\alpha_\omega) + \omega(G_{top} + \kappa_p + 2\lambda)\sin(\alpha_\omega)}A_{\mathcal{U},\omega}. \tag{16}$$

The top rotary reflection coefficient is defined as

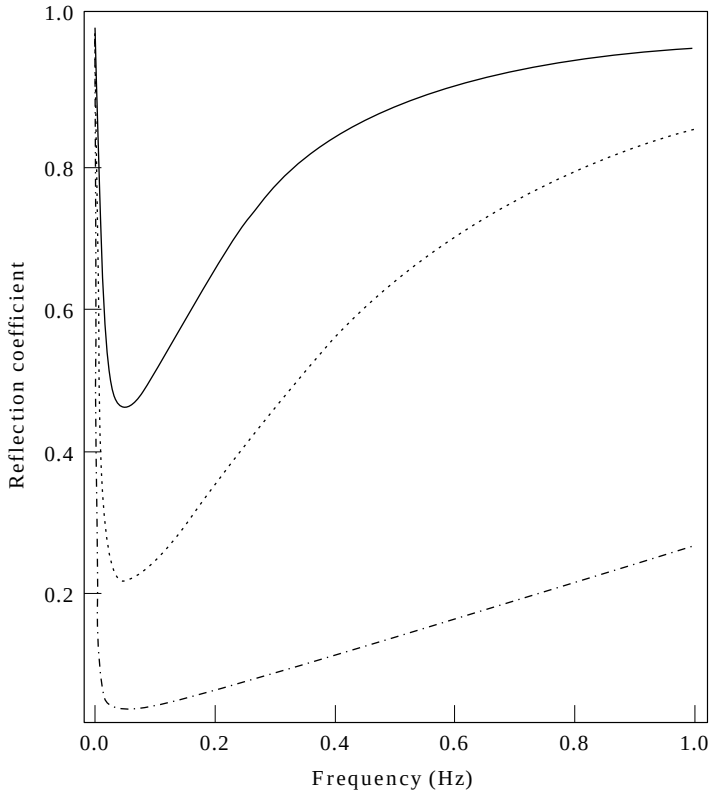

Figure 2. Variation of the top reflection coefficient as a function of frequency of incident torsional waves on the rotary from below using base data set 1. The top most curve corresponds to a zero torsional rectification control parameter. As the torsional rectification feedback is increased the reflection coefficient tends to uniformly decrease corresponding to increased absorption of torsional vibration. Key: —, $\lambda = 0$; $\cdots$, $\lambda = 1$; $-\cdot-\cdot$, $\lambda = 10$.

$$r_\omega \equiv |A_{\mathcal{D},\omega}/A_{\mathcal{U},\omega}| = \sqrt{(\omega^4 + a\omega^2 + \kappa_i^2)/(\omega^4 + b\omega^2 + \kappa_i^2)}, \tag{17}$$

where

$$a = (G_{top} - \kappa_p)^2 - 2\kappa_i, \quad b = (G_{top} + \kappa_p + 2\lambda)^2 - 2\kappa_i. \tag{18, 19}$$

The smaller the value of the reflection coefficient the greater the absorption of torsional vibration at the rotary. The shape of r_ω as a function of ω is hollow for $b - a > 0$. This is the situation here since $b - a = 4(G_{top} + \lambda)(\kappa_p + \lambda) > 0$ as G_{top} κ_p and λ are non-negative. In addition r_ω decreases monotonically with λ. Thus for any operational point a decrease in reflected torsional energy from the rotary can be achieved by increasing the control parameter λ. This is demonstrated in Figures 2 and 3. Each plot refers to a different data set describing the parameters κ_p, κ_i, G_{top}.

It follows that $0 < r_\omega \leqslant 1$ for any $0 \leqslant \omega$ and that $r_\omega \to 1$ as $\omega \to 0$ or ∞. Furthermore there is a unique minimum of r_ω when $\omega = \sqrt{\kappa_i}$. For any ζ $(0 < \zeta < 1)$ it is possible to arrange λ, κ_p, κ_i so that $r_\omega \leqslant \zeta$ for the spectral domain

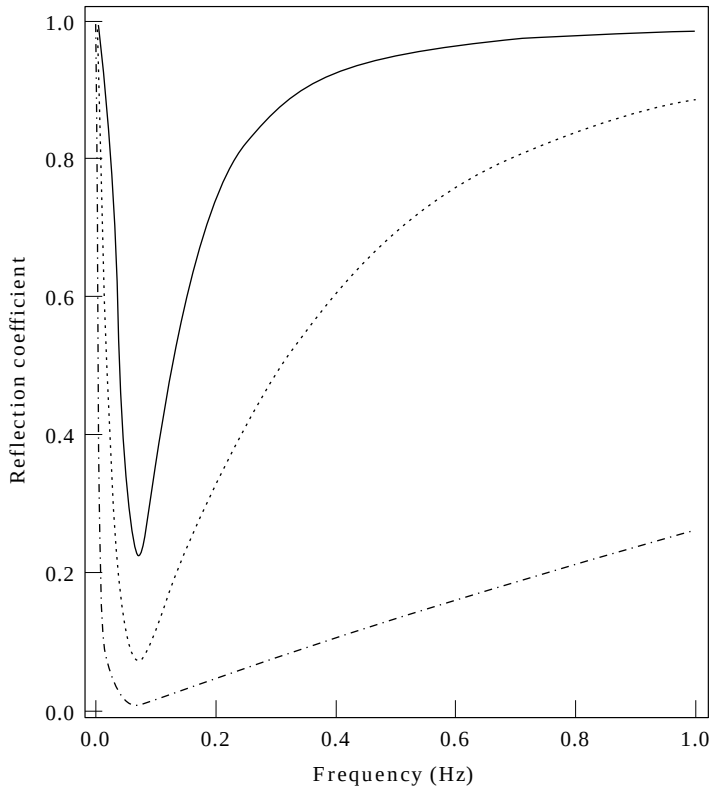

Figure 3. Variation of the top reflection coefficient as a function of frequency of incident torsional waves on the rotary from below using base data set 2. The top most curve corresponds to a zero torsional rectification control parameter. As the torsional rectification feedback is increased the reflection coefficient tends to uniformly decrease corresponding to increased abosrption of torsional vibration. Key as for Figure 2.

$0 \leqslant \omega_1 \leqslant \omega \leqslant \omega_2$. This can be achieved by choosing

$$\kappa_i = \omega_1 \omega_2$$

$$\lambda = -\tfrac{1}{2}(G_{top} + \kappa_p) + \frac{1}{2\zeta}\sqrt{(1-\zeta^2)(\omega_2 - \omega_1)^2 + (G_{top} - \kappa_p)^2}, \tag{20}$$

for any given κ_p. Thus one may control the amount of vibrational energy absorbed by the rotary within an assigned spectral domain. This is demonstrated in Figures 4 and 5 for $\zeta = 0{\cdot}2$ and $\omega_2 = 2$ ($\omega_1 = \kappa_i/\omega_2$). Each plot refers to a different data set describing the parameters κ_p, κ_i, G_{top}.

In the standard speed controller with $\lambda = 0$ equation (20) implies

$$(1-\zeta^2)\kappa_p^2 - 2G_{top}(1+\zeta^2)\kappa_p + (1-\zeta^2)(G_{top}^2 + (\omega_2 - \omega_1)^2) = 0, \tag{21}$$

which only yields real solutions for κ_p if

$$\omega_2 - \omega_1 \leqslant 2\zeta G_{top}/(1-\zeta^2). \tag{22}$$

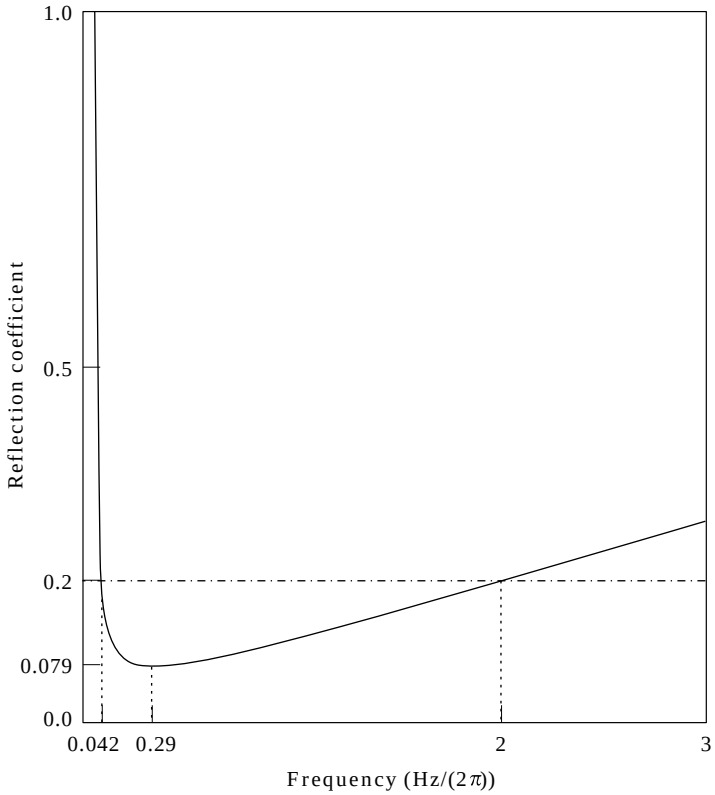

Figure 4. The extreme dotted vertical lines select a spectral window for absorption of torsional waves incident on the rotary from below. Using base parameter set 1 the torsional rectification control value is optimised to maintain 80% absorption over the whole spectral window. Note that this implies a minimum reflection at 0·29 Hz less than 8% in the region of torsional slip–stick oscillations. $\lambda = 4{\cdot}3$.

This can be a severe constraint since a small reflection coefficient ζ demands only a narrow frequency band for absorption.

It is interesting to observe how the additional control can be accommodated within the existing speed control provided the top torque conditions are approximately stationary. This means

$$|\ddot{\phi}(\sigma, \eta)| \ll 1. \tag{23}$$

It follows from equation (8) that

$$\phi'(0, \eta) \approx -(1/G_{top}) T_{motor}(\eta). \tag{24}$$

Therefore one may solve equation (12) together with equation (7) for T_{motor}:

$$\begin{aligned} T_{motor}(\eta) &= [G_{top}/(G_{top} + \lambda)](\kappa_p \dot{\xi}(\eta) + \kappa_i \xi(\eta) + \lambda \dot{\phi}(0, \eta)) \\ &= \underline{\kappa}_p \dot{\underline{\xi}}(\eta) + \underline{\kappa}_i \underline{\xi}(\eta), \end{aligned} \tag{25}$$

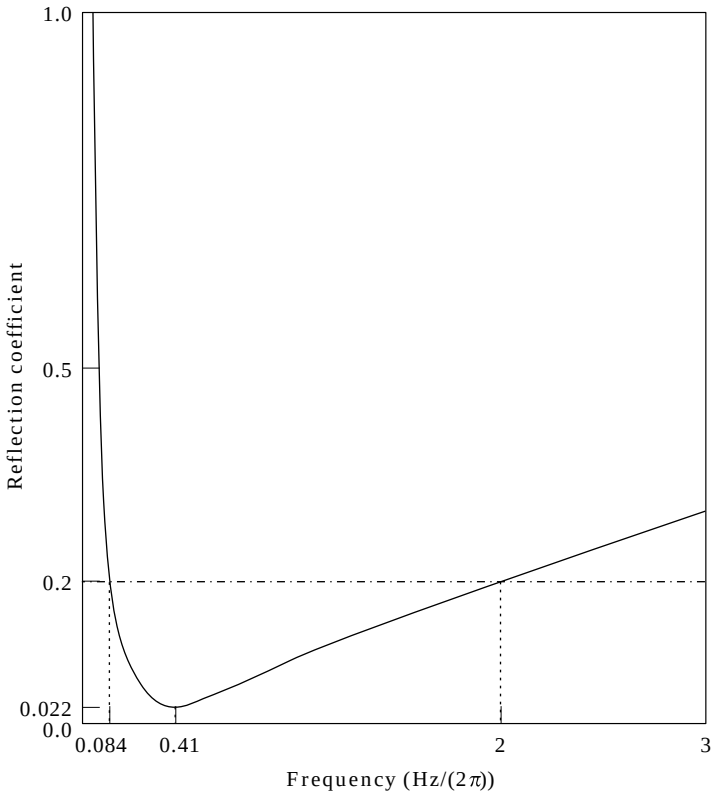

Figure 5. The extreme dotted vertical lines select a spectral window for absorption of torsional waves incident on the rotary from below. Using base parameter set 2 the torsional rectification control value is optimised to maintain 80% absorption over the whole spectral window. Note that this implies a minimum reflection at 0·41 Hz less than 3% in the region of torsional slip–stick ocillations. $\lambda = 4{\cdot}3$.

where

$$\underline{\kappa}_p = G_{top}(\kappa_p + \lambda)/(G_{top} + \lambda), \quad \underline{\kappa}_i = G_{top}\kappa_i/(G_{top} + \lambda) \tag{26, 27}$$

$$\underline{\xi}(\eta) = \Omega_0\eta - \phi(0, \eta) + \xi_0 - \lambda\Omega_0/\kappa_i = \xi(\eta) - \lambda\Omega_0/\kappa_i, \tag{28}$$

$$\dot{\underline{\xi}}(\eta) = \Omega_0 - \dot{\phi}(0, \eta) = \dot{\xi}(\eta). \tag{29}$$

Thus in this regime the effective integral and proportional gain parameters depend on λ in a well-defined way. However as noted above such a control procedure would be limited by the narrow band absorption of vibrational energy at the rotary.

3. SOFT-TORQUE

It is of interest to compare the present proposed control with the universally adopted soft-torque mechanism as the authors understand it [8]. This is obtained by modifying the standard speed controller by a high-pass filtered torque signal.

Thus the drive torque is given by

$$T_{motor}(\eta) = \kappa_p \dot{\xi}(\eta) + \kappa_i \xi(\eta), \tag{30}$$

where

$$\dot{\xi}(\eta) = \Omega_0 - hT_f(\eta) - \dot{\phi}(0, \eta), \tag{31}$$

$$\xi(\eta) = \Omega_0 \eta - h \int^{\eta} T_f(\tau)\, \mathrm{d}\tau - \phi(0, \eta) + \xi_0 \tag{32}$$

for some constant ξ_0 and control parameter h. In these expressions T_f is defined by

$$T_f(\eta) \equiv T_{contact}(\eta) - T_c(\eta), \tag{33}$$

where T_c is the output from a low-pass filter applied to the contact torque

$$T_{contact}(\eta) = -G_{top}\phi'(0, \eta) \tag{34}$$

measured at the rotary. A simple AC low-pass filter is described by the equation

$$\dot{T}_c(\eta) = \omega_c(T_{contact}(\eta) - T_c(\eta)), \tag{35}$$

where ω_c is the cut-off angular frequency. One may express the control in terms of T_c. Since

$$\int^{\eta} T_f(\tau)\, \mathrm{d}\tau = \frac{1}{\omega_c} \int^{\eta} \dot{T}_c(\tau)\, \mathrm{d}\tau = \frac{1}{\omega_c} T_c(\eta), \tag{36}$$

if follows that

$$\xi(\eta) = \Omega_0 \eta - (h/\omega_c) T_c(\eta) - \phi(0, \eta) + \xi_0. \tag{37}$$

As before, one seeks a solution of the form

$$\phi(\sigma, \eta) = A_{\mathcal{U},\omega} \sin(\omega(\eta + \sigma)) + A_{\mathcal{D},\omega} \sin(\omega(\eta - \sigma) + \alpha_\omega) + C_0 \sigma + \Omega_0 \eta, \tag{38}$$

describing incident harmonic waves reflected from the rotary. The constants C_0, α_ω and the ratio $A_{\mathcal{D}}/A_{\mathcal{U}}$ follow from the conditions (8), (30)–(35). A somewhat involved calculation yields the results

$$C_0 = -\omega_c \xi_0 \kappa_i / G_{top}(h\kappa_i + \omega_c), \tag{39}$$

$$\alpha_\omega = \tan^{-1}([a_1\omega^5 + a_2\omega^3 + a_3\omega]/[a_4\omega^6 + a_5\omega^4 + a_6\omega^2 + a_7]), \tag{40}$$

with

$$a_1 = -2G_{top}, \quad a_2 = -2G_{top}(-\kappa_i + h\kappa_i G_{top} - h\kappa_p \omega_c G_{top} + \omega_c^2),$$

$$a_3 = 2G_{top}\kappa_i \omega_c^2, \quad a_4 = 1,$$

$$a_5 = 2\kappa_i(hG_{top} - 1) + \omega_c^2 - 2h\kappa_p\omega_c G_{top} + \kappa_p^2(hG_{top} - 1)^2 - G_{top}^2,$$

$$a_6 = \kappa_i^2(hG_{top} - 1)^2 - 2\kappa_i\omega_c^2 + \omega_c^2(\kappa_p^2 - G_{top}^2), \quad a_7 = \kappa_i^2\omega_c^2.$$

and

$$A_{\mathcal{D},\omega}/A_{\mathcal{U},\omega} = 1/[\cos(\alpha_\omega) + F(\omega)\sin(\alpha_\omega)], \tag{41}$$

where

$$F(\omega) = (Q_1\omega^3 + Q_2\omega)/(A\omega^4 + B\omega^2 + C) \tag{42}$$

$$A = 1, \quad B = hG_{top}(\kappa_i - \omega_c\kappa_p) - \kappa_i + \omega_c^2, \quad C = -\kappa_i\omega_c^2,$$

$$Q_1 = G_{top}(h\kappa_p - 1) - \kappa_p, \quad Q_2 = G_{top}\omega_c(h\kappa_i - \omega_c) - \kappa_p\omega_c^2.$$

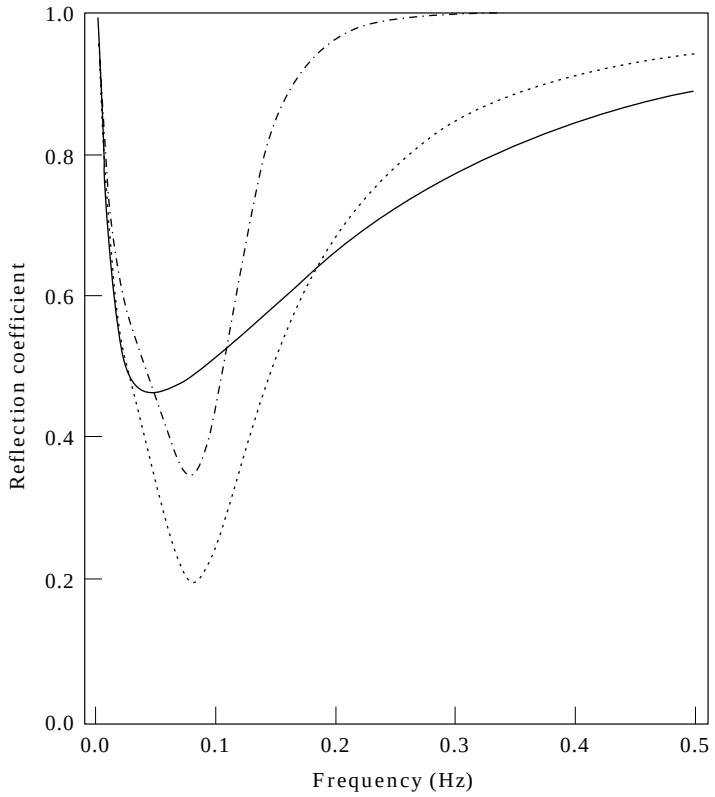

Figure 6. Variation of the top reflection coefficient as a function of frequency of incident torsional waves on the rotary from below using base data set 1. The curve with greatest lower bound corresponds to a zero soft-torque control parameter. As the soft-torque control feedback parameter is increased the reflection coefficient minima do not uniformly decrease. The absorption of torsional vibration is therefore not a uniform function of the soft-torque feedback control. Key: —, $h = 0$; · · · ·, $h = 1{\cdot}2$; – · – · , $h = 2{\cdot}1$.

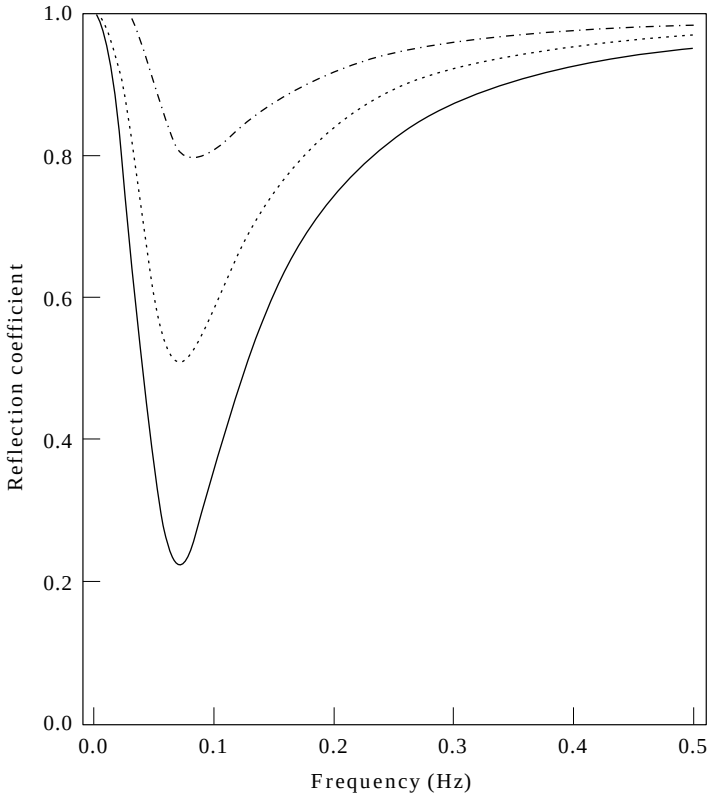

Figure 7. Variation of the top reflection coefficient as a function of frequency of incident torsional waves on the rotary from below using base data set 2. The curve with lowest bound corresponds to a zero soft-torque control parameter. As the soft-torque control feedback parameter is increased the reflection coefficient minima in this case actually increase. The absorption of torsional vibration is therefore reduced rather than increased by increasing the soft-torque feedback. Key: —, $h = 0$; · · · ·, $h = 0{\cdot}7$; – · – · , $h = 1{\cdot}2$.

Figures 6 and 7 demonstrate the variation of the reflection coefficient as a function of frequency for various values of the soft-torque control parameter h. Each figure refers to different sets of field parameters as before. *By contrast to the torsional rectification control the shape of the reflection coefficient curves no longer varies uniformly with h*. In Figure 6, the minimum initially decreases before increasing with increasing h. In Figure 7, increasing h from a zero value (corresponding to a situation with soft-torque control off) produces only an increased reflection at all frequencies. This dramatic behaviour may help to explain the volatility of effective soft-torque control. It also demonstrates the superiority of control by torsional rectification.

As has been noticed in the previous section if the top torque conditions are approximately stationary the contact torque can be approximated by the motor torque according to equations (23) and (24). The corresponding phase shift and the reflection coefficient of an incident torsional harmonic wave on the rotary have the same form as in equations (40–42) with the following substitutions:

$$a_1 = -2G_{top}(1 + \kappa_p h)^2,$$

$$a_2 = -2G_{top}(\omega_c^2 + h(2\kappa_i - \kappa_p^2)\omega_c + \kappa_i(\kappa_i h^2 - 1)),$$

$$a_3 = 2G_{top}(\kappa_i\omega_c^2 + \omega_c\kappa_i^2 h), \quad a_4 = (1 + \kappa_p h)^2,$$

$$a_5 = \omega_c^2 - (1 + \kappa_p h)^2 G_{top}^2 + 2h(\kappa_i - \kappa_p^2)\omega_c - 2\kappa_i + \kappa_i^2 h^2 + \kappa_p^2,$$

$$a_6 = (\kappa_p^2 - 2\kappa_i)\omega_c^2 - (\omega_c + \kappa_i h)^2 G_{top}^2 - 2\omega_c\kappa_i^2 h + \kappa_i^2, \quad a_7 = \kappa_i^2\omega_c^2,$$

$$A = (1 + \kappa_p h)^2, \quad B = (\kappa_i h + \omega_c)^2 - h\omega_c\kappa_p^2 - \kappa_i, \quad C = -\omega_c\kappa_i(\kappa_i h + \omega_c),$$

$$Q_1 = G_{top}(1 + \kappa_p h)^2 + \kappa_p(1 + \kappa_p h), \quad Q_2 = (\kappa_i h + \omega_c)^2 G_{top} + \kappa_i^2 h + \kappa_p\omega_c^2.$$

Furthermore the variation of the reflection coefficient as a function of frequency for various values of the soft-torque control parameter h in such an approximation has a similar behaviour as demonstrated in Figures 6 and 7. Thus circumventing the feedback of contact torque in this manner would only be effective in a narrow frequency band of torsional vibration.

4. CONTROL OF TORSIONAL SLIP–STICK OSCILLATIONS

The previous sections have outlined the general ideas leading to the control of vibrational absorption by torque feedback at the rotary. The reflection coefficient frequency characteristics have been determined by regarding the bit interaction with the rock surface as a source of torsional disturbances. To see the effects of the bit dynamics on a finite drill-string one must examine the complete dynamical system and take into account the non-linear bit-torque frictional reaction that is largely responsible for the antidamping and excitation of torsional relaxation oscillations (slip–stick). A model that accommodates the complex non-linear dynamics of a one dimensional continuum in space subject to dynamic boundary conditions has been developed in reference [11] based on a simple Cosserat model and the exact geometrical formulation of elasticity established in [12].

If one ignores axial and lateral motion of the drill-string the dynamics are determined by a solution $\phi(\sigma, \eta)$ to equation (1) describing the angular position of the drill-string segment at location σ and time η and satisfying boundary conditions at each end. The drill-string is attached to the top drive at $\sigma = 0$ and to the BHA at $\sigma = 1$. With the abbreviations $\Phi_T(\eta) := \phi(0, \eta)$, $\Phi_B(\eta) := \phi(1, \eta)$, $\Phi'_T(\eta) := (\partial\phi/\partial\sigma)(0, \eta)$, $\Phi'_B(\eta) := (\partial\phi/\partial\sigma)(1, \eta)$, the boundary conditions are obtained by balancing the torques at each end of the drill-string:

$$\ddot{\Phi}_T - G_{top}\Phi'_T - T_{motor}(\Phi_T, \Phi'_T, \dot{\Phi}_T, \eta) = 0, \quad \ddot{\Phi}_B + G_{bit}\Phi'_B + \mathcal{F}(\dot{\Phi}_B) = 0, \quad (43, 44)$$

where $\mathcal{F}$ describes the torque friction at the bit and the effective moments of

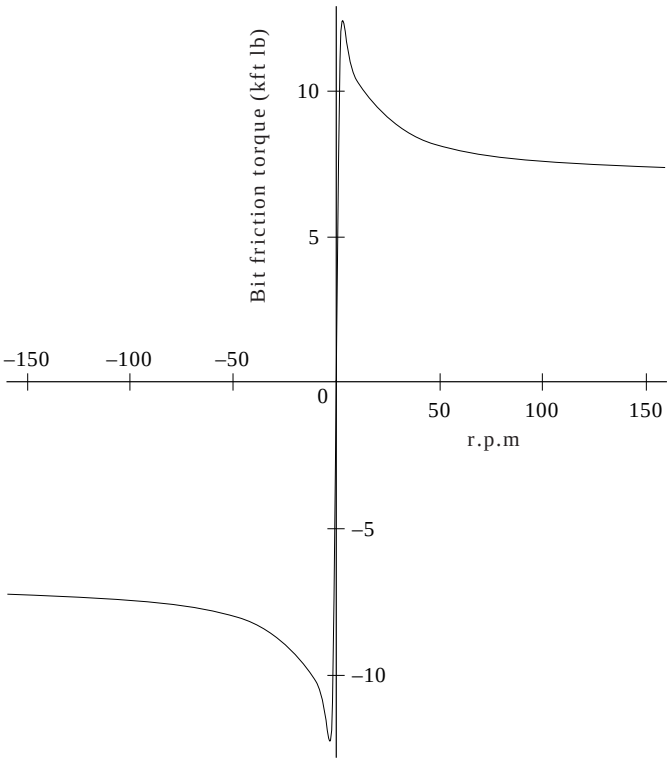

Figure 8. The excitation of torsional relaxation vibrations leading to the phenomena of slip–stick is determined by antidamping characteristics induced by non-linear torque-friction between the active drill-bit and the rock formation. The above profile simulates the frictional torque experienced in the field operation with base parameter set 2. The steep regions of the profile determine the duration and characteristics of the so called "stick" phase of the rotary motion of the drill-bit.

inertia of the top drive and BHA respectively have been scaled into the coupling constants G_{top} and G_{bit}.

In this context the simplest approximation is to ignore the finite time of propagation of torsional waves along the drill-string and treat the system as a simple forced torsional pendulum under non-linear damping at the bit. In such an approximation one ignores the excitation of all axial and lateral vibrations in the system and replaces the full spectrum of torsional excitations of the drill-string by a simple torsional spring that couples the torque from the top-drive with the torque generated between the bit and the rock surface, $(\Phi'_T \simeq \Phi_T - \Phi_B)$. This model has been used in references [10, 13] to discuss the stability of the linearised system in the space of the operating parameters in the presence of a simple speed controller with parameters κ_p, κ_i. In the present case the system additionally includes the previously discussed torque feedback with the parameter λ for torsional rectification control or h for soft-torque control. The equations of motion for the torsional displacement Φ_T at the top and Φ_B at the bit then take the form:

$$\ddot{\Phi}_T + G_{top}(\Phi_T - \Phi_B) - T_{motor}(\Phi_T, \Phi_B, \dot{\Phi}_T, \eta) = 0, \tag{45}$$

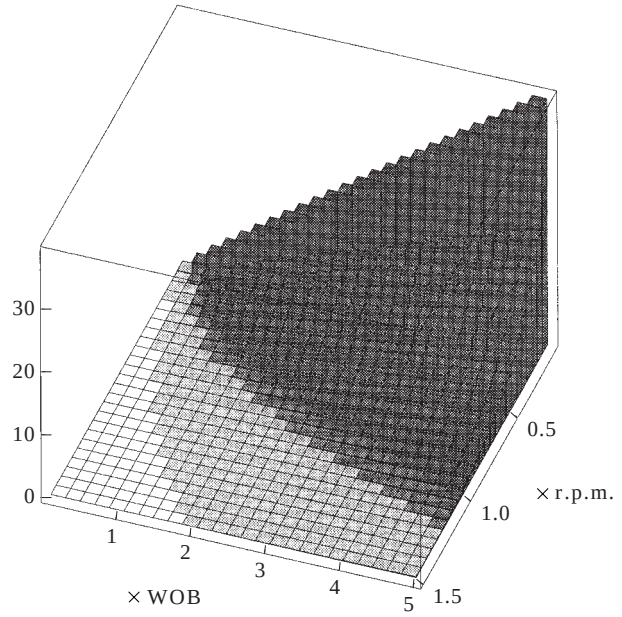

Figure 9. The active drill system can excite a number of characteristic vibrational modes. The frequency and lifetime of instabilities are encoded in the roots of the characteristic system associated with a linearisation about a stationary target configuration. The figure displays the pure torsional vibrational spectrum for base data set 2 ($\lambda = 0$) as a function of target rotary speed and "weight on bit" (WOB). The white domains indicate the absence of excitable unstable modes and correspond to "torsionally safe" drilling configurations. The vertical blocks indicate the presence of unstable torsional vibrations. The height of each block indicates the reciprocal of the life-time (in seconds) of the most unstable mode in this domain. The frequencies are grey coded and increase with the darkness level.

$$\ddot{\Phi}_B + G_{bit}(\Phi_B - \Phi_T) + \mathcal{F}(\dot{\Phi}_B) = 0. \tag{46}$$

Figure 8 displays the dependence of bit-torque friction $\mathcal{F}$ on the rotary speed of the bit $\dot{\Phi}_B$ in r.p.m. corresponding to a "weight on bit" typical of a value in the field operation with base parameter set 2. The essential torsional instability arises from linearizations about target angular speeds Ω_0 where the effective bit-friction torque has antidamping characteristics.

Figures 9–17 display the stability characteristics for such a model based on linearizations about stationary configurations as a function of target r.p.m. and "weight on bit" based on operations with base parameter set 2. Figures 9–13 refer to the proposed torsional rectification control while Figures 14–17 permit a comparison with conventional soft-torque control.

Each horizontal axis is labelled by the factor multiplying values of either typical target r.p.m. or nominal "weight on bit". In Figure 9 the operational regime with base factor co-ordinates (1, 1) lies on the border between stability and instability. A small increase in torsional rectification feedback parameter in subsequent plots shows how the operational regime then moves into full stability. Each plot corresponds to a different control parameter. The height of

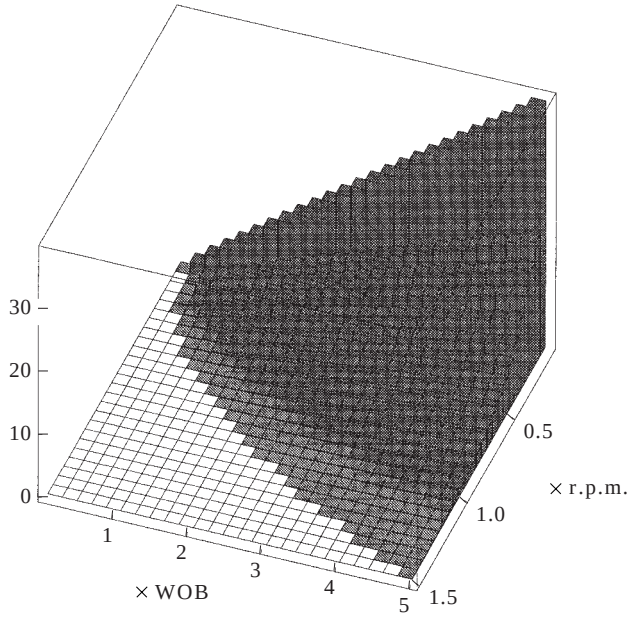

Figure 10. The figure displays the pure torsional vibration spectrum with increased torsional rectification feedback in operation. The figure displays the pure torsional vibrational spectrum for base data set 2 ($\lambda = 0{\cdot}5$) as a function of target rotary speed and "weight on bit" (WOB). The white domains and vertical block height have the significance described in Figure 9.

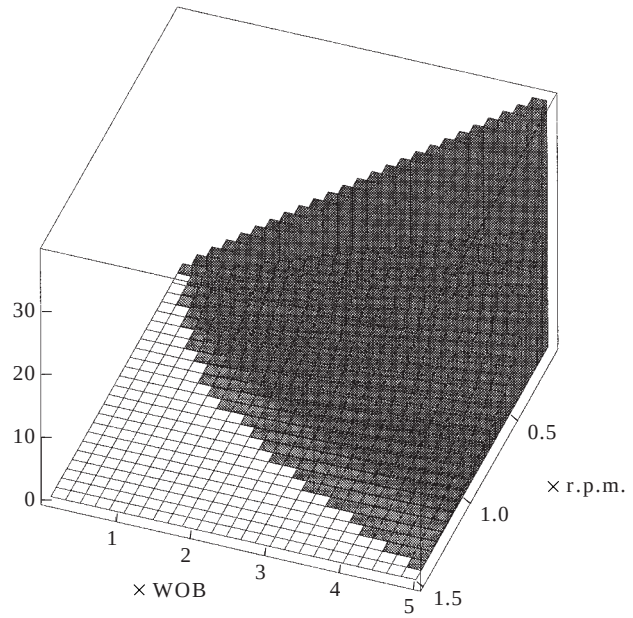

Figure 11. The figure displays the pure torsional vibration spectrum with increased torsional rectification feedback in operation. The figure displays the pure torsional vibrational spectrum for base data set 2 ($\lambda = 1$) as a function of target rotary speed and "weight on bit" (WOB). The white domains and vertical block height have the significance described in Figure 9.

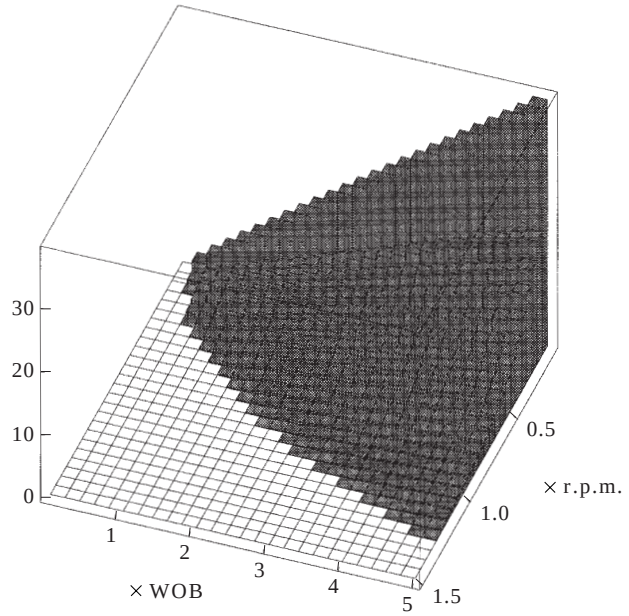

Figure 12. The figure displays the pure torsional vibration spectrum with increased torsional rectification feedback in operation. The figure displays the pure torsional vibrational spectrum for base data set 2 ($\lambda = 10$) as a function of target rotary speed and "weight on bit" (WOB). The white domains and vertical block height have the significance described in Figure 9.

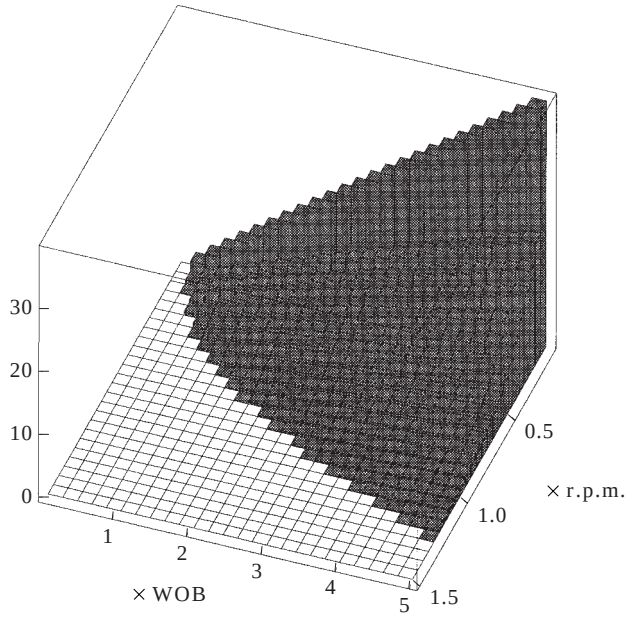

Figure 13. The figure displays the pure torsional vibration spectrum with increased torsional rectification feedback in operation. The figure displays the pure torsional vibrational spectrum for base data set 2 ($\lambda = 50$) as a function of target rotary speed and "weight on bit" (WOB). The white domains and vertical block height have the significance described in Figure 9.

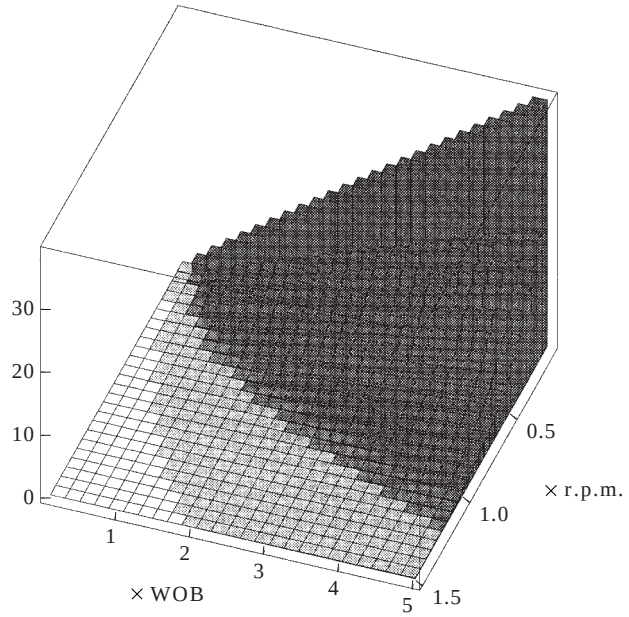

Figure 14. The figure displays the pure torsional vibration with soft-torque feedback off. The figure displays the pure torsional vibration spectrum for base data set 2 ($h = 0$) as a function of target rotary speed and "weight on bit" (WOB). The white domains and vertical block height have the significance described in Figure 9.

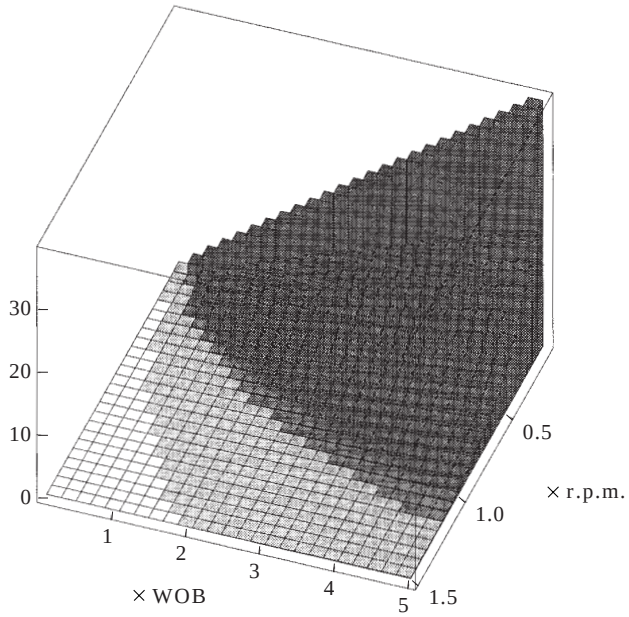

Figure 15. The figure displays the pure torsional vibration spectrum with increased soft-torque feedback in operation. The figure displays the pure torsional vibrational spectrum for base data set 2 ($h = 0{\cdot}03$) as a function of target rotary speed and "weight on bit" (WOB). The white domains and vertical block height have the significance described in Figure 9.

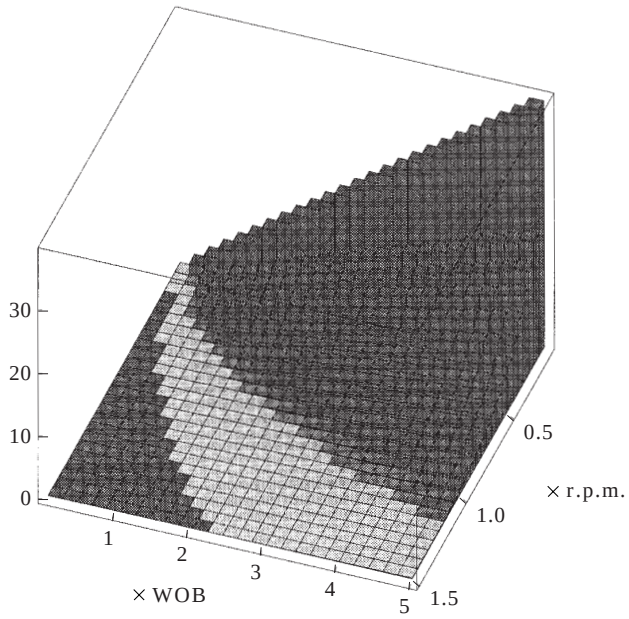

Figure 16. The figure displays the pure torsional vibration spectrum with increased soft-torque feedback in operation. The figure displays the pure torsional vibrational spectrum for base data set 2 ($h = 0{\cdot}1$) as a function of target rotary speed and "weight on bit" (WOB). The white domains and vertical block height have the significance described in Figure 9.

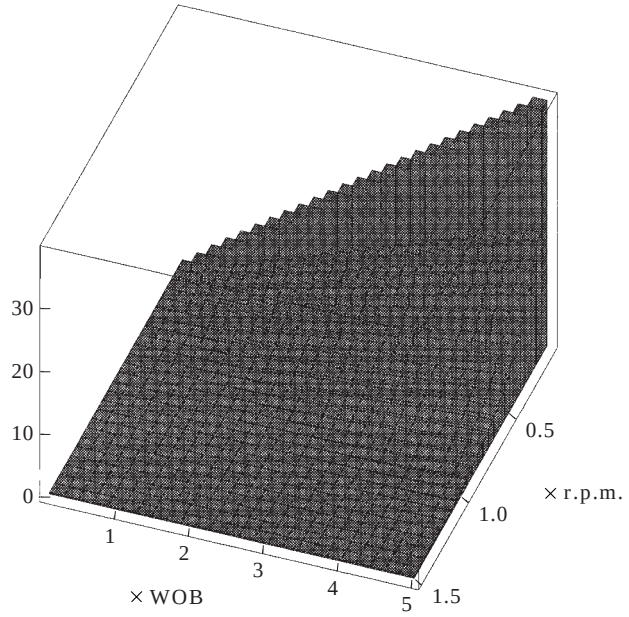

Figure 17. The figure displays the pure torsional vibration spectrum with increased soft-torque feedback in operation. The figure displays the pure torsional vibrational spectrum for base data set 2 ($h = 1$) as a function of target rotary speed and "weight on bit" (WOB). The dark domains indicate the presence of excitable unstable modes and correspond to "unsafe" drilling configurations. The vertical blocks indicate the presence of unstable torsional vibrations. The height of each block indicates the reciprocal of the life-time (in seconds) of the most unstable mode in this domain.

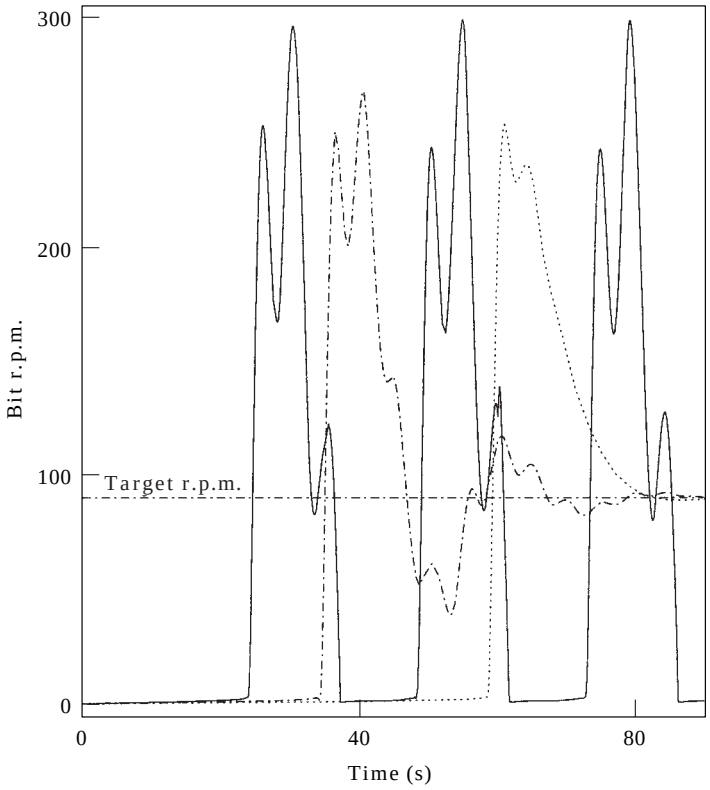

Figure 18. This figure exhibits the predictions of bit r.p.m. as a function of time from a simple model simulation (based on data set 2) that exhibits slip–stick oscillations in the absence of torque feedback. The results of three simulations are superimposed. The removal of unwanted oscillations is clearly evident with increasing torque rectification feedback. Key: —, $\lambda = 0$; – · – ·, $\lambda = 0{\cdot}3$; · · · ·, $\lambda = 1$.

each block corresponds to the time constant in reciprocal seconds for the growth of the most unstable torsional mode. Thus the taller the plot the more unstable the domain. White domains denote stable working regions for torsional perturbations.

It will be noticed that as the soft-torque parameter h is increased the white domains of stability are considerably less than the corresponding domains of stability obtained by increasing the torsional rectification control parameter λ and total instability rapidly occurs. This is consistent with the predictions based on the analysis of the rotary reflection coefficient above and augers well for the elimination of slip–stick triggered by dynamic bit-friction. To explore the effects of torsional rectification for *arbitrary torsional displacements* the equations above can be integrated numerically without recourse to linearisation. A dynamical simulation is performed with this simple non-linear model in a dynamical environment where slip–stick is evident in the absence of soft-torque or rectification control. In Figure 18 the results of three simulations of the dynamical bit r.p.m. as a function of time are superimposed for increasing values

of the torsional rectification control parameter λ. The rapid elimination of the torsional slip–stick is clear, in full accord with the linearised stability predictions.

To accommodate the effects of torsional wave propagation along a finite length of drill-string subject to dynamic boundary conditions reference [14] requires a considerably more sophisticated simulation model [11]. For axisymmetric configurations (including axial vibrations) the general conclusion above is maintained. The more general model [11] suggests that the efficacy of all forms of torsional control is limited by the inherent instabilities induced by lateral vibrations of the drill-string and its associated interactions with the wall of the borehole.

5. CONCLUSION

A method of controlling torsional relaxation oscillations of an active drilling assembly has been explored in two simple models. In the first model the absorption of monochromatic torsional waves at the rotary of a drilling assembly, generated by a prescribed source of up-moving waves at the drill-bit was explored using the fact that torsional waves satisfy a simple wave equation when vibrating in an axially symmetric configuration. In the second model the finite time of propagation of the torsional waves along the drill-string was ignored and the system regarded as a simple forced torsional pendulum but with non-linear torques generated by the drill-bit. In both cases the superiority of the torsional rectification method proposed here over conventional control techniques has been demonstrated.* Although it is probably true that, if control is limited to torque feedback from the top-drive, one cannot fundamentally prevent the bit from reacting to non-linear friction and acting as a source of upward moving torsional waves, by measuring the dynamic contact torque proportional to the spatial derivative of the twist of the drill-string as near as possible to the rotary, an improved torque feedback control can be constructed. The authors believe that, with relatively minor investment in the application of transducers capable of actively measuring both torsional speed and contact torque at the rotary, a more robust controller could be constructed by combining existing speed controllers with torsional rectification control (as prescribed in (7)) thereby leading to a significant improvement of drilling operations.

ACKNOWLEDGMENT

We are most grateful to F. Abbassian, M. Fear, S. Parfitt and J. Schray for their valuable advice in this investigation and to the Levehulme Trust, EPSRC and BP for financial support.

*The advantages of eliminating torsional relaxation oscillations by torsional rectification control over conventional soft-torque control indicated in the simple models above have been subsequently born out in the presence of torsional wave propagation [16]. Torsional rectification offers a more robust control environment leading to a greatly expanded torsional stability regime compared with conventional controls.

REFERENCES

1. P. Sananikone, O. Kamoshima and D. B. White 1992 *Proceedings of the IADC/SPE Drilling Conference*, *New Orleans*, *Paper* 23891. A field method for controlling drill-string torsional vibrations.
2. A. Tondl 1975 *Journal of Sound and Vibration* **42**, 251–260. Quenching of self-excited vibrations: equilibrium aspects.
3. J. F. Brett 1991 *SPE/IADC Drilling Conference*, *Amsterdam*, *Paper* 21943. The genesis of bit-induced torsional drill-string vibrations.
4. V. A. Dunayevsky, F. Abbassian and A. Judziz 1993 *SPE Drilling and Completion,* 84–92. Dynamic stability of drill-strings under fluctuating weight on bit.
5. S. V. Belokobyl'skii and V. K. Prokopov 1982 *Soviet Applied Mechanics* **18**, 1134–1138. Friction-induced self-excited vibrations of drill-rig with exponential drag law.
6. M. P. Dufeyte and H. Henneuse 1991 *SPE/IADC Drilling Conference*, *Amsterdam*, *Paper* 21945. Detection and monitoring of the slip–stick motion: field experiments.
7. R. P. Dawson, Y. Q. Lin and P. D. Spanos 1987 *Spring Conference of the Society for Experimental Mechanics*, *Houston*. Drill string slip–stick oscillations.
8. G. W. Halsey, A. Kyllingstad and A. Kylling 1988 *Proceedings of the* 63*rd SPE Annual Technical Conference and Exhibition*, *Houston*, *Paper* 18049. Torque feedback used to cure slip–stick motion.
9. M. J. Fear and F. Abbassian 1994 *SPE* 28908, 433–448. Experience in the detection and suppression of torsional vibration from mud logging data.
10. J. D. Jansen and L. van den Steen 1995 *Journal of Sound and Vibration* **179**, 647–668. Active damping of self-excited torsional vibrations in oil well drill-strings.
11. R. W. Tucker and C. Wang 1999 *Journal of Sound and Vibration* (to appear). An integrated model for drill-string dynamics.
12. S. Antman 1991 *Non-linear Problems in Elasticity*, *Applied Mathematical Sciences* 107. Berlin: Springer-Verlag.
13. V. A. Dunayevsky and F. Abbassian 1995 *BP Technical Report*, *SPE* 30478. Application of stability approach to bit dynamics.
14. J. Schray and R. W. Tucker 1995 *Lancaster University Report*. The stability of extended string models.
15. R. W. Tucker and C. Wang 1997 *http://www.lancs.ac.uk/users/SPC/Physics.htm*. The excitation and control of torsional slip–stick in the presence of axial vibrations.
16. S. Parfitt, R. W. Tucker and C. Wang 1999 Lancaster University report. Guidelines from the Cosserat dynamics of a drilling assembly.